

# Linear Poroelastic Cancellous Bone Anisotropy: Trabecular Solid Elastic and Fluid Transport Properties

**Sean S. Kohles**

ASME Member,  
Kohles Bioengineering,  
1731 SE 37th Ave,  
Portland, OR 97214-5135;  
Department of Mechanical Engineering,  
Oregon State University,  
Corvallis, OR

**Julie B. Roberts**

TEI Biosciences, Inc.,  
7 Elkins St,  
Boston, MA 02127

*The mechanical performance of cancellous bone is characterized using experiments which apply linear poroelasticity theory. It is hypothesized that the anisotropic organization of the solid and pore volumes of cancellous bone can be physically characterized separately (no deformable boundary interactive effects) within the same bone sample. Due to its spongy construction, the in vivo mechanical function of cancellous or trabecular bone is dependent upon fluid and solid materials which may interact in a hydraulic, convective fashion during functional loading. This project provides insight into the organization of the tissue, i.e., the trabecular connectivity, by defining the separate nature of this biphasic performance. Previous fluid flow experiments [Kohles et al., 2001, Journal of Biomechanics, 34(11), pp. 1197–1202] describe the pore space via orthotropic permeability. Ultrasonic wave propagation through the trabecular network is used to describe the solid component via orthotropic elastic moduli and material stiffness coefficients. The linear poroelastic nature of the tissue is further described by relating transport (fluid flow) and elasticity (trabecular load transmission) during regression analysis. In addition, an empirical relationship between permeability and porosity is applied to the collected data. Mean parameters in the superior-inferior (SI) orientation of cubic samples ( $n=20$ ) harvested from a single bovine distal femur were the largest ( $p<0.05$ ) in comparison to medial-lateral (ML) and anterior-posterior (AP) orientations: Apparent elastic modulus (2,139 MPa), permeability ( $4.65 \times 10^{-10} \text{ m}^2$ ), and material stiffness coefficient (13.6 GPa). A negative correlation between permeability as a predictor of structural elastic modulus supported a parametric relationship in the ML ( $R^2=0.4793$ ), AP ( $R^2=0.3018$ ), and SI ( $R^2=0.6445$ ) directions ( $p<0.05$ ). [DOI: 10.1115/1.1503374]*

## 1 Introduction

Within the structural hierarchy of cancellous bone, it can be represented as biphasic in nature. The combination of trabecular rods-plates and a hierarchical pore space filled with viscous fluid and vascular tissue creates a complex mechanical response during loading [1–4]. Any contributions to the apparent modulus or yield strength via “hydraulic stiffening” may arise from the containment of the internal fluid by the cortical shell or the trabecular matrix itself. However, this effect has not been fully characterized and is most likely associated with small dynamic time scales [5]. Within linear poroelasticity theory, the unique biphasic mechanical loading response within this bony tissue is described by: 1) the large difference in bulk moduli between the solid and fluid components and 2) small local tissue deformations [6]. This performance should not be confused with the biphasic descriptions of soft tissues (similar solid/fluid moduli and large deformations) [7]. Describing the properties of the distinct volumetric spaces (solid and porous) may provide some insight into their functional interaction during mechanical loading.

The mechanical and transport properties of bone have been described as highly dependent upon orientation and anatomical location [8–11]. The inter-connectivity of the trabecular network defines the spatial [12–14] and directional [15,16] dependencies that influence the structural elasticity. These descriptions are usually defined with respect to principal trabecular orientations as well as primary anatomic directions.

Bone structural anisotropies have also been characterized using

fluid dynamics via streaming potentials, traces, and flow visualization [17–21]. The mechanics of the internal fluid have been described [22–25] as dependent upon functional pressure differentials during structural loading [26]. The characteristic of this convective mass transfer is dependent upon the shape of the available space for flow [27,28]. Ultimately this fluid flow affects the state of bone cells (osteocytes) and is a component of the biologic mechanosensory system proposed [29] for the cellular maintenance or degeneration of tissue via osteoblasts and osteoclasts.

The objective of this study was to investigate the relationships between the structural anisotropic, elastic and transport properties of cancellous bone in the primary anatomic directions in such a way as to minimize hydraulic interactions (as described by finite deformation theory). This application of linear elasticity theory and biphasic characterization requires that the pore space be characterized without mechanically influencing the solid component. In addition, the trabecular solid properties must be quantified without altering the pore space boundary. This resulting information will contribute to the development of anisotropic poroelasticity experimental protocols [30] and help to test the validity of linear poroelastic theory as a descriptor of cancellous bone.

## 2 Methods

**2.1 Parametric Relationships.** Experimental techniques were designed to characteristically isolate the pore and solid spaces without functional interaction (linear poroelasticity) based upon the following parametric descriptions. Transport phenomena can be used to describe fluid ( $\mu$ ) flow through the open pore

Contributed by the Bioengineering Division for publication in the JOURNAL OF BIOMECHANICAL ENGINEERING. Manuscript received July 2001; revised manuscript received June 2002. Associate Editor: R. Vanderby Jr.

volume ( $A_{pore}$ ) within a length ( $L$ ) of bone. Flow ( $Q$ ) due to an applied pressure ( $p$ ) and can be described by permeability ( $k$ ) using Darcy's Law:

$$k = \frac{Q\mu L}{\rho A_{pore} p} \quad (1)$$

An analogous description can be applied using elasticity to describe load transmission through the solid volume ( $A_{solid}$ ) within a length ( $L$ ) of bone. Solid deformation ( $\Delta L$ ) or strain ( $\varepsilon$ ) due to an applied force ( $F$ ) or stress ( $\sigma$ ) can be described by elastic modulus ( $E$ ) using Hooke's Law:

$$E = \frac{\sigma}{\varepsilon} = \frac{FL}{\Delta LA_{solid}} \quad (2)$$

Thus direct and inverse relationships are apparent between terms when comparing the analogous systems described by these coefficients (equations (1) and (2)) which appear in constitutive equations. Relationships are noted for permeability and elastic modulus and their respective effort variables ( $p$  and  $F$ ) and flow variables ( $Q$  and  $\Delta L$ ) used to describe the fluid and solid phases [31]. These descriptions are not affected or constrained by the interaction between the phases (fluid pressure does not deform the solid nor does solid deformation pressurize the fluid) [30,32]. Thus independent measurements without interaction may be achieved with the experimental application of low-pressure, direct perfusion and low-force, ultrasonic wave propagation.

**2.2 Tissue Preparation.** A two-tailed power analysis conducted on preliminary permeability and elasticity data from unidirectional ( $n=6$  cylinders) and multidirectional ( $n=4$  cubes) experiments [33,34], determined that testing a minimum of 19 samples would provide the strength necessary to identify the statistical influence of orientation ( $\alpha-1=95\%$ ). Twenty cubic samples (mean volume  $\pm$  standard deviation =  $4.09 \text{ cm}^3 \pm 0.13$ ) were harvested from a single bovine distal femoral condyle age 18–24 months. Anatomic orientation and origin were recorded during the harvesting procedure. The samples were cleaned through iterations of soaking (water, trichloroethylene), ultrasonication, airjetting, and centrifugation. Details of the harvesting and cleaning procedures have been previously described [35]. An Archimedes's displacement technique was used to determine a homogenized pore volume, porosity ( $P$ ), irrespective of cross-sectional orientation.

**2.3 Transport Properties.** The intrinsic permeability ( $k_i$ ) of each bone sample was measured using a previously reported experimental technique [35] based upon fluid flow through porous media described by Eq. (1):

$$k_i = \frac{\dot{m}_i L_i \mu}{\rho A \Delta p} \quad (3)$$

for mass flow rate ( $\dot{m}_i$ ), sample length ( $L_i$ ), fluid viscosity ( $\mu$ ), fluid density ( $\rho$ ), pore cross-sectional area ( $A$ ), and the pressure gradient across the sample ( $\Delta p$ ). Three tests were conducted in each of three orthogonal directions, for  $i$ =Medial-Lateral (ML), Anterior-Posterior (AP), and Superior-Inferior (SI), on all twenty cubes for a total of 180 permeability tests. For transport measurements, water ( $\rho_{\text{water}} = 1.00 \text{ g/cm}^3$ ,  $\mu_{\text{water}} = 1.00 \text{ cp}$  at  $20^\circ\text{C}$ ) flowed from an elevated reservoir to a collection reservoir. A minimal hydrostatic pressure differential ( $\Delta p = 1744 \text{ Pa}$ ) was maintained through each bone sample. The mass flow rate was acquired continuously from the collection reservoir using a digital scale (Ohaus Navigator 800, Florham Park, NJ) and a PC-based virtual instrument (LabView, National Instruments, Corp., Austin, TX).

In addition to direct measurements, an empirical relationship between permeability and porosity was approximated using the Kozeny equation [5,36,37]:

$$k(P) = \frac{C \cdot P^3}{S_V(P)^2} \quad (4)$$

The surface area to sample volume ratio ( $S_V$ ) was calculated assuming that the measured pore volume for each cancellous cube was comprised of intertrabecular void spaces, spherical in shape with a characteristic lineal dimension of up to 1 mm [6,35]. The "Kozeny constant" ( $C$ ), a void shape parameter, was numerically adjusted to fit the permeability and porosity measurements (see Data Analysis below).

**2.4 Elastic Properties.** The anisotropic elastic moduli of the cancellous structure ( $E_i$ ) and the trabecular material stiffness coefficients ( $c_i$ ) were calculated using an ultrasound pulse transmission technique demonstrated previously [38]. This technique characterizes the effect of load transmission through the tissue, as identified by equation (2), while minimizing the effects of tissue deformation ( $\Delta L \approx 0$ ) and thus valid for characterizing linear poroelasticity theory. The apparent density ( $\rho_a = \rho_m(1-P)$ ) and the solid material density ( $\rho_m$ ) were determined for each sample. Propagation velocities ( $v_i$ ) were then measured with sending and receiving longitudinal wave transducers, a pulser-receiver (Model 5058PR, Panametrics, Waltham, MA), and a multichannel oscilloscope (Model TDS460A, Tektronix, Beaverton, OR). System delays were determined and accounted for during the measurement of propagation times [34]. Longitudinal transducers with a frequency of 100 kHz (Model X1020, Panametrics) were used to find the structural (or apparent) elastic moduli:

$$E_i = \rho_a v_i^2 \quad (5)$$

where the wavelength of the propagating wave ( $\lambda > 15 \text{ mm}$ ) is longer than the sample dimension (long wavelength theory) as validated in earlier work [39]. Longitudinal wave transducers with a frequency of 10 MHz (Model V112, Panametrics) were applied to determine the trabecular material stiffness coefficients:

$$c_i = \rho_m v_i^2 \quad (6)$$

The use of Eq. (6) assumes that the wavelength of the propagating wave ( $\lambda < 0.3 \text{ mm}$ ) is near the size of a trabecula and the propagating distance between transducers follows a straight trabecular path. There is some error in the application of Eq. (6) to samples with a bone volume fraction of less than 1.0. Comparisons between columnar oriented trabeculae and randomly oriented trabeculae demonstrated an error up to 45% for similar (95% confidence interval of 61.4% to 72.2%) porosity values [40]. We assume that the error encountered here will be much less than 45% due to sample orientation which is coincident with anatomic orientation and thus an assumed orthotropic symmetry. Three measurements in each of the three orthogonal directions ( $i$  = ML, AP, and SI) using the two sets of transducers were conducted on all twenty cubes for 360 total ultrasound measurements.

**2.5 Data Analysis.** Two-factor analysis of variance (ANOVA) was applied to all collected data to explore the effects of tissue heterogeneity and anisotropy as predictors of elastic and transport properties (Statview v5.0, SAS Institute, Inc., Cary, NC). Linear and nonlinear regression analysis was also applied to test parametric relationships. Statistical significance was assumed for all comparisons with a  $p < 0.05$ . The empirical Kozeny permeability equation was fit to the permeability versus porosity data. The "Kozeny constant" ( $C$ ) was solved to minimize the root mean square (RMS) error between the calculated and measured average permeability values using a generalized reduced gradient, nonlinear optimization code (Excel 2000, Microsoft, Redmond, WA).

### 3 Results

All elastic and transport parameters demonstrated an overall statistical dependence on measurement direction ( $p < 0.05$ ) while independent of anatomic location ( $p > 0.05$ ). Consistently, the highest mean values ( $\pm$  standard deviation) of apparent elastic

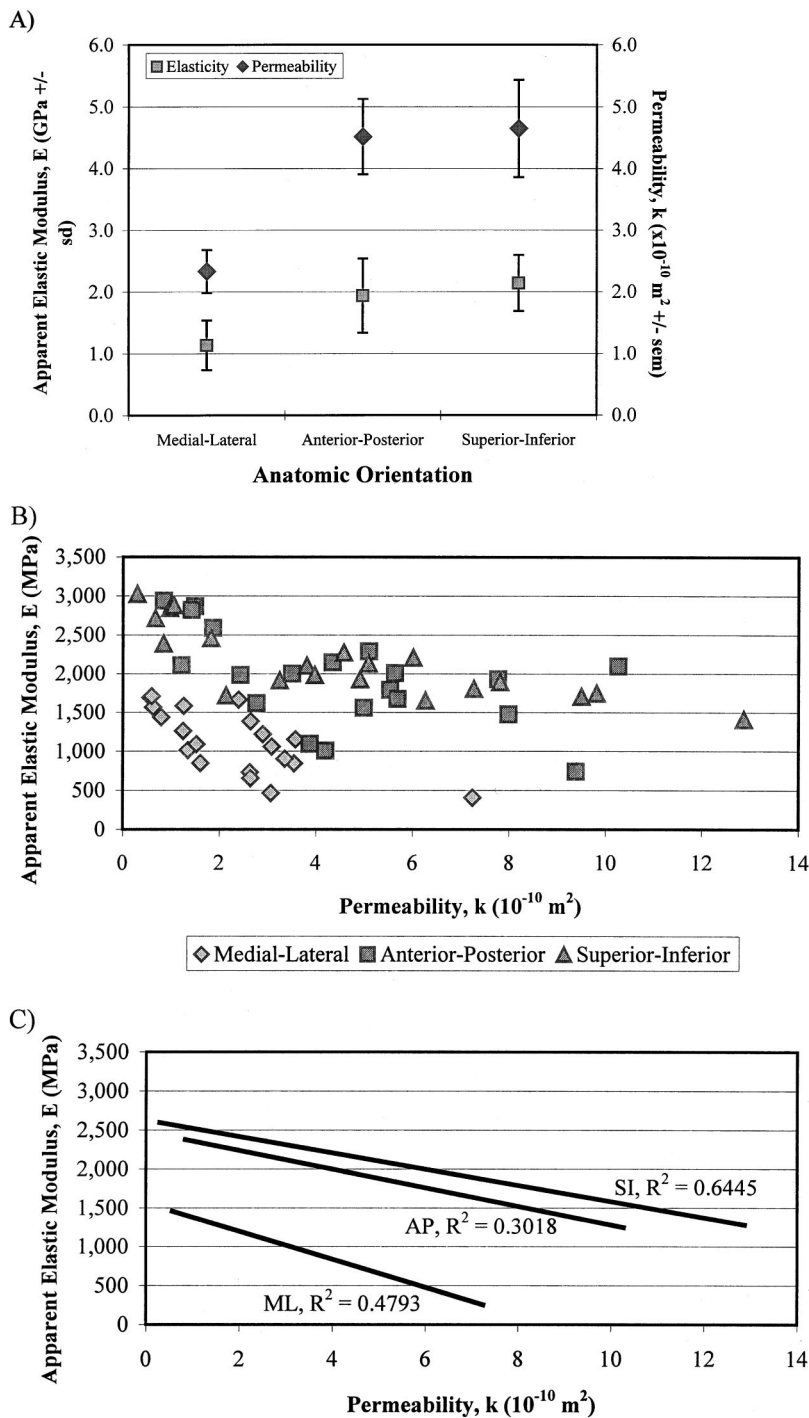


**Fig. 1** The relationship between anisotropic, apparent elastic moduli and transport properties in bovine cancellous bone. The plots show: **A)** the mean and error values (standard deviation, sd, or standard error of the mean, sem) for modulus and permeability; **B)** the orthotropic data for all samples ( $n = 20$ ); and **C)** the linear trendlines with coefficients that are statistically different than zero ( $p < 0.5$ ) for the three orientations (when combined,  $R^2 = 0.0405$ ). Permeability values were originally presented in Kohles et al. [35].

modulus ( $2,139 \pm 455$  MPa) and permeability ( $4.65 \times 10^{-10} \pm 3.50 \times 10^{-10}$  m<sup>2</sup>) were measured in the SI direction (Fig. 1A). These SI values were statistically similar to AP direction values ( $p > 0.05$ ) in addition to being statistically greater than the ML direction values ( $p < 0.05$ ). Although parametrically related, the negative correlation between permeability as a predictor of structural elastic modulus (Figs. 1B and 1C) varied in the ML

( $R^2 = 0.4793$ ), AP ( $R^2 = 0.3018$ ), and SI ( $R^2 = 0.6445$ ) directions ( $p < 0.05$ ). The influence of porosity on elastic modulus (Fig. 2A) and permeability (Fig. 2B) indicated strong relationships. A Kozeny constant ( $C = 0.022$ ), as an indicator of void shape, was determined by minimizing the error between the predicted and calculated permeabilities ( $RMS = 1.99 \times 10^{-10}$  m<sup>2</sup>). Trabecular material stiffness was also higher in the SI direction ( $13.6 \pm 3.0$

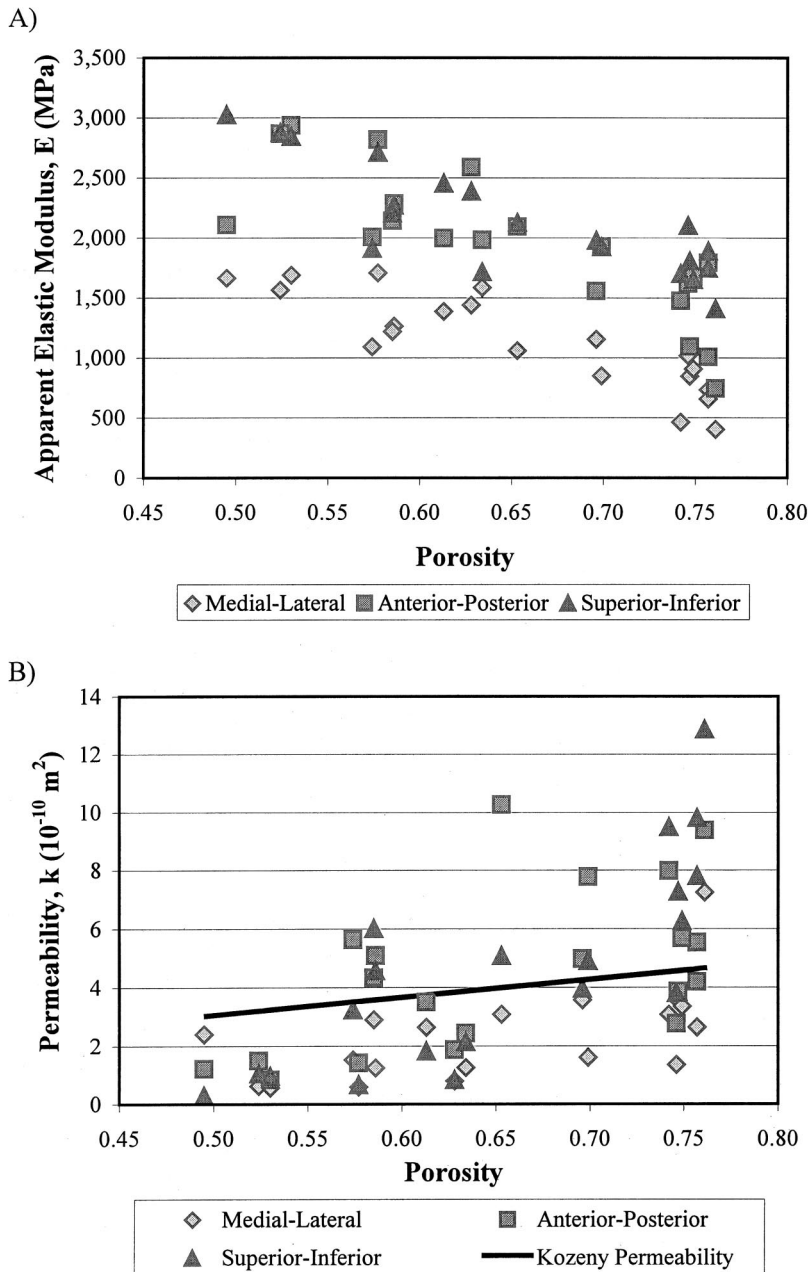


Fig. 2 A graphical comparison between porosity as a predictor of: A) apparent elastic moduli and B) permeability. The Kozeny equation was fit to the permeability versus porosity data as a means to empirically describe this relationship ( $C=0.022$ , equation 4).

GPa) in comparison with the ML ( $p < 0.05$ ,  $7.93 \pm 2.54$  GPa) and AP ( $p > 0.05$ ,  $12.50 \pm 2.78$  GPa) directions (Fig. 3) and was positively correlated as a predictor of structural modulus ( $R^2 = 0.3172$ ).

#### 4 Discussion

In this study, the anisotropy of cancellous bone was characterized through the use of two distinct measurement techniques. The use of low-level fluid pressures and ultrasonic wave propagation experiments provided the means to minimize hydraulic biphasic couplings and thus measure linear poroelastic mechanical parameters within single cubic bone samples. The experimental setup was designed to enforce the assumption that the boundaries of the elastic porous solid do not move due to the loading environment.

This movement would be on the order of the displacement gradients squared but has been neglected, as in linear elasticity theory.

The resulting orthotropic values were consistent with those produced in distinct elasticity [8] and transport [9,10] investigations. Structural elastic modulus of bovine cancellous bone in superior-inferior orientations was found to be slightly higher than that determined by Njeh et al. [41] (1,195 MPa) and Ashman et al. [39] (1,158 MPa). Reported material stiffness coefficient values, which are a measure of the trabecular solid elasticity, were similar to moduli of individual trabeculae for bovine bone described by Ashman and Rho [42] (10.9 GPa) as well as human bone described by Ashman and Rho [42] (13.0 GPa) and Rho et al. [43] (14.8 GPa). Cancellous bone permeabilities were within the same order of magnitude reported by others and summarized previously [35].



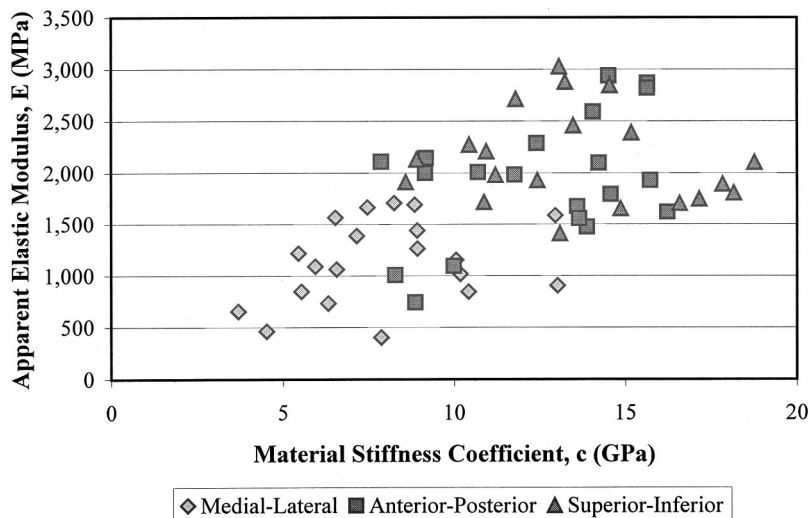


**Fig. 3** The relationship between anisotropic, apparent elastic moduli and material stiffness coefficients. A linear regression applied to the combined data results in a positive correlation with  $R^2=0.3172$ .

A utility of the presented techniques is in the potential to complement finite element modeling and examine functional adaptation issues. With recent advances in micro computed tomography and computational systems, small-scale modeling has become more accurate in its description of cancellous bone function [44]. A variety of mechanical evaluation techniques are currently being applied to distinguish apparent and material properties while considering solid-phase anisotropy [45–47]. Validation of the available models [48], while examining structural hierarchies and time-dependent changes in tissue organization, can strengthen both the accuracy of a particular model's results as well as its potential therapeutic application.

The direct measurements of cancellous bone poroelastic coefficients described here can be used to predict some of the fluid-solid functional parameters derived via consolidation mechanical testing [40]. This technique may also provide a preliminary assessment of anisotropy [49] as a precursor to mechanical evaluation along principal axes of symmetry. Poroelasticity or consolidation theory provides a constitutive relationship explicitly relating the strain contributions of the solid phase and fluid phase due to an applied load environment [6]. Drained and undrained, triaxial compression testing are required to characterize the components of the compliance matrix and the effects on pore pressure [30,50]. This testing regimen has been used for multiaxial evaluation of trabecular failure [51] although complete experimental characterization of the poroelastic constitutive relationship is as yet forthcoming.

This paper describes the ability to nondestructively quantify structural and material properties in multiple orientations within a single bone sample without deformation-induced hydraulic effects. This characterization can provide an initial assessment of poroelastic anisotropy before applying more rigorous mechanical testing as well as contribute to phenomenological and/or computational descriptions of cancellous bone structure-function [52].

### Acknowledgments

The authors recognize the valuable contributions of Dr. Lawrence Bonassar, Christopher Wilson, Maureen Upton, Alyssa Schlichting, Laura Cooper, and Rebecca Thibeault including the constructive comments from Daniel Young, Dr. Peder Pedersen, and Dr. Allen Hoffman. Partial support for this project was provided by the Department of Biomedical Engineering and the Of-

fice for Academic Affairs at Worcester Polytechnic Institute, Worcester, MA, as well as through a Special Opportunities Award from the Whitaker Foundation.

### References

- [1] Carter, D. R. and Hayes, W. C., 1977, "The Compressive Behavior of Bone as a Two-Phase Porous Structure," *J. Bone Jt. Surg.*, **59A**, pp. 954–962.
- [2] Simkin, P. A., Houghlum, S. J., and Pickereil, C. C., 1985a, "Compliance and Viscoelasticity of Canine Shoulders Loaded in vitro," *J. Biomech.*, **18**, p. 735–743.
- [3] Keaveny, T. M., and Hayes, W. C., 1993, "A 20-Year Perspective on the Mechanical Properties of Trabecular Bone," *ASME J. Biomech. Eng.*, **115**, pp. 534–542.
- [4] Ochoa, J. A., Sanders, A. P., Kiesler, T. W., Heck, D. A., Toombs, J. P., Brandt, K. D., and Hillberry, B. M., 1977, "In vivo Observations of Hydraulic Stiffening in the Canine Femoral Head," *ASME J. Biomech. Eng.*, **119**, pp. 103–108.
- [5] Arramon, Y. P., and Cowin, S. C., 1997, "Hydraulic Stiffening of Cancellous Bone," *Forma*, **12**, pp. 209–221.
- [6] Cowin, S. C., 1999, "Bone poroelasticity," *J. Biomech.*, **32**, pp. 217–238.
- [7] Mow, V. C., Kuei, S. C., and Lai, W. L., 1980, "Biphasic Creep and Stress Relaxation of Articular Cartilage in Compression: Theory and Experiments," *ASME J. Biomech. Eng.*, **102**, pp. 73–84.
- [8] Ashman, R. B., Rho, J. Y., and Turner, C. H., 1989, "Anatomical Variation of Orthotropic Elastic Moduli of the Proximal Tibia," *J. Biomech.*, **22(8–9)**, pp. 895–900.
- [9] Grimm, M. J., and Williams, J. L., 1997, "Measurements of Permeability in Human Calcaneal Trabecular Bone," *J. Biomech.*, **30(7)**, pp. 743–745.
- [10] Nauman, E. A., Fong, K. E., and Keaveny, T. M., 1999, "Dependence of Intertrabecular Permeability on Flow Direction and Anatomic Site," *Ann. Biomed. Eng.*, **27**, pp. 517–524.
- [11] Giesen, E. B. W., Ding, M., Dalstra, M., van Eijden, T. M. G. J., 2001, "Mechanical Properties of Cancellous Bone in the Human Mandibular Condyle are Anisotropic," *J. Biomech.*, **34(6)**, pp. 799–803.
- [12] McKelvie, M. L., and Palmer, S. B., 1991, "The Interaction of Ultrasound with Cancellous Bone," *Phys. Med. Biol.*, **36**, pp. 1331–1340.
- [13] Tavakoli, M. B., and Evans, J. A., 1992, "The Effect of Bone Structure on Ultrasonic Attenuation and Velocity," *Ultrasonics*, **30**, pp. 389–395.
- [14] Hosokawa, A., and Otani, T., 1997, "Ultrasonic Wave Propagation in Bovine Cancellous Bone," *J. Acoust. Soc. Am.*, **101**, pp. 558–562.
- [15] Williams, J. L., and Lewis, J. L., 1982, "Properties and an Anisotropic Model of Cancellous Bone from the Proximal Tibial Epiphysis," *J. Biomech. Eng.*, **104**, pp. 50–56.
- [16] Williams, J. L., and Johnson, W. J. H., 1989, "Elastic Constants of Composites Formed from PMMA Bone Cement and Anisotropic Bovine Tibial Cancellous Bone," *J. Biomech.*, **22**, pp. 673–682.
- [17] Pollack, S. R., Petrov, N., Salzstein, R., Brankov, G., and Blagoeva, R., 1984, "An Anatomical Model for Streaming Potentials in Osteons," *J. Biomech.*, **17(8)**, pp. 627–636.
- [18] Wehrli, F. W., Ford, J. C., Chung, H. W., Wehrli, S. L., Williams, J. L., Grimm, M. J., Kugelmass, S. D., and Jara, H., 1993, "Potential Role of Nuclear Mag-

- netic Resonance for the Evaluation of Trabecular Bone Quality," *Calcif. Tissue Int.*, **53**, S162–S169.
- [19] Schemitsch, E. H., Kowalski, M. J., and Swiontkowski, M. F., 1994, "Evaluation of a Laser Doppler Flowmetry Implantable Fiber System for Determination of Threshold Thickness for Flow Detection in Bone," *Calcif. Tissue Int.*, **55**, pp. 216–222.
- [20] MacGinitie, L. A., Stanley, G. D., Bieber, W. A., and Wu, D. D., 1997, "Bone Streaming Potentials and Currents Depend on Anatomical Structure and Loading Orientation," *J. Biomech.*, **30**(11–12), pp. 1133–1139.
- [21] Wang, L., Cowin, S. C., Weinbaum, S., and Fritton, S. P., 2000, "Modeling Tracer Transport in an Osteon Under Cyclic Loading," *Ann. Biomed. Eng.*, **28**, pp. 1200–1209.
- [22] Bryant, J. D., 1983, "The Effect of Impact on the Marrow Pressure of Long Bone in vitro," *J. Biomech.*, **16**, pp. 659–665.
- [23] Simkin, P. A., Pickerell, C. C., and Wallis, W. J., 1985b, "Hydraulic Resistance in Bones of the Canine Shoulder," *J. Biomech.*, **18**, pp. 657–663.
- [24] Downey, D. J., Simkin, P. A., and Taggart, R., 1988, "The Effect of Compressive Loading on Intraosseous Pressure in the Femoral Head in vitro," *J. Bone Jt. Surg.*, **70A**, pp. 871–877.
- [25] Ochoa, J. A., Sanders, A. P., Heck, D. A., and Hillberry, B. M., 1991, "Stiffening of the Femoral Head Due to Intertrabecular Fluid and Intraosseous Pressure," *J. Biomech. Eng.*, **113**, pp. 259–262.
- [26] Kohles, S. S., and Vanderby, Jr., R., 1997, "Thermographic Strain Analysis of the Proximal Canine Femur," *Med. Eng. Phys.*, **19**, pp. 262–266.
- [27] Dillman, R. M., Roer, R. D., and Gay, D. M., 1991, "Fluid Movement in Bone: Theoretical and Empirical," *J. Biomech.*, **24**, pp. S163–S177.
- [28] Hui, P. W., Leung, P. C., and Sher, A., 1996, "Fluid Conductance of Cancellous Bone Graft as a Predictor for Graft-Host Interface Healing," *J. Biomech.*, **29**, pp. 123–132.
- [29] Cowin, S. C., 1986, "Wolff's Law of Trabecular Architecture at Remodeling Equilibrium," *J. Biomech. Eng.*, **108**, pp. 83–88.
- [30] Young, D. W., and Kohles, S. S., 2001, "Experimental Determination of bone Anisotropic Poroelasticity Parameters," *Proc. 27th Annual Northeast Bioengineering Conference*, **27**, pp. 41–42.
- [31] Johnson, A. T., 1999, *Biological Process Engineering: An Analogical Approach to Fluid Flow, Heat Transfer, and Mass Transfer Applied to Biological Systems*, John Wiley & Sons, Inc., New York.
- [32] Thompson, M., and Willis, J. R., 1991, "Reformation of the Equations of Anisotropic Poroelasticity," *ASME J. Appl. Mech.*, **58**, pp. 612–616.
- [33] Kohles, S. S., Roberts, J. B., Upton, M. L., Wilson, C. G., Schlichting, A. L., Cooper, L. J., Thibeault, R. A., and Bonassar, L. J., 2000, "Anisotropic Elastic and Transport Properties of Cancellous Bone," *Ann. Biomed. Eng.*, **28**(S1), p. S6.
- [34] Roberts, J. B., 2000, "Anisotropic Elastic and Transport Properties of Cancellous Bone," Masters Thesis, Worcester Polytechnic Institute.
- [35] Kohles, S. S., Roberts, J. B., Upton, M. L., Wilson, C. G., Bonassar, L. J., and Schlichting, A. L., 2001, "Direct Perfusion Measurements of Cancellous Bone Anisotropic Permeability," *J. Biomech.*, **34**(11), pp. 1197–1202.
- [36] Scheidegger, A. E., 1974, *The Physics of Flow Through Porous Media*, University of Toronto Press, Toronto, Canada.
- [37] Kessler, D. P., and Greenkorn, R. A., 1999, *Momentum, Heat, and Mass Transfer Fundamentals*, Marcel Dekker, Inc., NY.
- [38] Kohles, S. S., Bowers, J. R., Vailas, A. C., and Vanderby, Jr., R., 1997, "Ultrasonic Wave Velocity Measurement in Small Polymeric and Cortical Bone Specimens," *J. Biomech. Eng.*, **119**(3), pp. 232–236.
- [39] Ashman, R. B., Corin, J. D., and Turner, C. H., 1987, "Elastic Properties of Cancellous Bone: Measurement by an Ultrasonic Technique," *J. Biomech.*, **20**(10), pp. 979–986.
- [40] Williams, J. L., 1992, "Ultrasonic Wave Propagation in Cancellous and Cortical Bone: Prediction of Some Experimental Results by Biot's Theory," *J. Acoust. Soc. Am.*, **91**(2), pp. 1106–1112.
- [41] Njeh, C. F., Hodgskinson, R., Currey, J. D., and Langton, C. M., 1996, "Orthogonal Relationships Between Ultrasonic Velocity and Material Properties of Bovine Cancellous Bone," *Med. Eng. Phys.*, **18**(5), pp. 373–381.
- [42] Ashman, R. B., and Rho, J. Y., 1998, "Elastic Modulus of Trabecular Bone Material," *J. Biomech.*, **21**(3), pp. 177–181.
- [43] Rho, J. Y., Ashman, R. B., and Turner, C. H., 1993, "Young's Moduli of Trabecular and Cortical Bone Material: Ultrasonic and Microtensile Measurements," *J. Biomech.*, **26**, pp. 111–119.
- [44] van Rietbergen, B., 2001, "Micro-FE Analyses of Bone: State of the Art," *Adv. Exp. Med. Biol.*, **496**, 21–30.
- [45] Bourne, B. C., Morgan, T. G., Paschalis, E. P., and van der Meulen, M. C., 2002, "Cancellous Bone Anisotropy Arises from both Architecture and Material Properties," *Trans. 48th Annual Orthopaedic Research Society Meeting*, **27**, p. 558.
- [46] Homminga, J., McCreadie, B. R., Ciarelli, T. E., Weinans, H., Goldstein, S. A., and Huiskes, R., 2002, "Trabecular Bone Mechanical Properties from Normals and Patients with Hip Fractures Differ on the Apparent Level, Not on the Tissue Level," *Trans. 48th Annual Orthopaedic Research Society Meeting*, **27**, p. 570.
- [47] Niebur, G., Yeh, O. C., and Keaveny, T. M., 2002, "Damage Evolution in Trabecular Bone is Anisotropic," *Trans. 48th Annual Orthopaedic Research Society Meeting*, **27**, p. 323.
- [48] Miller, Z., Fuchs, M. B., and Arcan, M., 2002, "Trabecular Bone Adaptation with an Orthotropic Material Model," *J. Biomech.*, **35**(2), pp. 247–256.
- [49] Kohles, S. S., Roberts, J. B., Upton, M. L., Wilson, C. G., Bonassar, L. J., Schlichting, A. L., 2001, "Anisotropic Elastic and Transport Properties of Cancellous Bone," *Trans. 47th Annual Orthopaedic Research Society Meeting*, **26**, p. 516.
- [50] Lim, T. H., and Hong, J. H., 2000, "Poroelastic Properties of Bovine Vertebral Trabecular Bone," *J. Orthop. Res.*, **18**(4), pp. 671–677.
- [51] Keaveny, T. M., Wachtel, E. F., Zadesky, S. P., and Arramon, Y. P., 1999, "Application of the Tsai-Wu Quadratic Multiaxial Failure Criterion to Bovine Trabecular Bone," *ASME J. Biomech. Eng.*, **121**(1), pp. 99–107.
- [52] Kohles, S. S., and Martinez, D. A., 2000, "Elastic and Physicochemical Relationships in Cortical Bone," *J. Biomed. Mater. Res.*, **49**(4), pp. 479–488.